**(Preprint) AAS 25-855**

# THE MODIFIED GENERALIZED EQUINOCTIAL ORBITAL ELEMENTS FOR HIGH-FIDELITY CISLUNAR PROPAGATION

**Maaninee Gupta*** **and Kyle J. DeMars†**

The complex cislunar dynamical environment poses challenges for spacecraft navigation and Space Domain Awareness operations, where the knowledge of current and future spacecraft states is essential. To accurately model the underlying dynamics, this work explores the Modified Generalized Equinoctial Orbital Elements to enable high-fidelity propagation for cislunar applications. The accuracy of the solutions is demonstrated via comparisons against Cartesian $n$-body solutions across various cislunar orbits. The characterization of uncertainty in generalized coordinates under high-fidelity propagation is compared against Cartesian methods.

## INTRODUCTION

With the recent interest in missions to the vicinity of the Moon, cislunar space is poised to become the domain that sustains humanity's presence beyond the Earth. With this renewed interest, Space Domain Awareness (SDA), that has conventionally applied to the sub-geosynchronous orbit domain, is necessary to support cooperative and safe operations in cislunar space as well. In contrast to SDA near the vicinity of the Earth, SDA in the broad volume of cislunar space presents unique challenges due to its vast size and significant distance from the Earth. In addition, the cislunar dynamical environment is characterized by non-Keplerian motion resulting from the non-negligible impact of lunar gravity perturbations. Thus, a dynamical model that captures the influence of both the Earth and the Moon, in addition to other perturbing forces, is necessary to represent cislunar dynamics.

The Earth-Moon Circular Restricted Three-Body Problem (CR3BP) is one option for a medium-fidelity dynamical model that accounts for the gravity of both the Earth and the Moon, a requisite for cislunar dynamics modeling. However, the CR3BP fails to account for the pulsation of the Earth-Moon distance, as well as other perturbations that are potentially significant for certain cislunar orbits, including solar gravity, solar radiation pressure, and the spherical harmonics for the Earth and the Moon. To accurately simulate the cislunar dynamical environment, it is necessary to be able to capture these additional perturbations without losing accuracy or increasing the complexity of the dynamical model.

The Generalized Equinoctial Orbital Elements (GEqOEs) provide an avenue for a low-complexity methodology to incorporate both conservative and non-conservative perturbations that manifest in cislunar space. The GEqOE set has been successfully leveraged for state and uncertainty propagation of near-Earth orbits with third-body perturbations and oblateness effects.[1,2] More recently,

*Postdoctoral Researcher, Department of Aerospace Engineering, Texas A&M University, College Station, TX 77843
†Associate Professor, Department of Aerospace Engineering, Texas A&M University, College Station, TX 77843

Gupta and DeMars have applied the GEqOEs for capturing three-body dynamical motion in cislunar space, with better preservation of Gaussian behavior for uncertainty propagated along various cislunar orbits.[3,4] The goal of the current work is to extend the applicability of the generalized coordinates for high-fidelity dynamical modeling in cislunar space. Cislunar orbits that are significantly impacted by the gravitational effects of the Earth, Moon, and Sun are propagated directly in the generalized coordinates. The accuracy of this methodology is validated through comparison against the $n$-body dynamical model based in Cartesian coordinates. In order to capture the varying levels of perturbations that arise across the cislunar domain, various orbits that span the volume of cislunar space are considered. In addition to high-fidelity state propagation, this work investigates the characterization of uncertainty in the generalized coordinates. The Bhattacharyya coefficient is employed to quantify the preservation of Gaussianity under high-fidelity dynamics, allowing a direct comparison against Cartesian state representations.

## HIGH-FIDELITY STATE PROPAGATION

In the current work, orbital motion is characterized in generalized coordinates, leveraging orbital element representations that capture all the necessary forces in the dynamical regime. Specifically, the Modified Generalized Equinoctial Orbital Elements (M-GEqOEs), an offshoot of the Generalized Equinoctial Orbital Elements (GEqOEs), are utilized for state and uncertainty propagation. While the GEqOE set demonstrates success in propagating various cislunar periodic orbits, its validity is restricted to trajectories characterized by a negative total energy.[3] The M-GEqOE set supplies the modifications necessary to overcome that limitation and improve the robustness of modeling trajectories in the cislunar domain. Details regarding the element sets are provided by Bau et al.[1] and Gupta et al.[5] for the GEqOEs and M-GEqOEs, respectively. An overview of the M-GEqOEs and their time derivatives, along with the methodology employed for modeling cislunar dynamics, is provided below.

### Modified Generalized Equinoctial Orbital Elements

The set of Modified Generalized Equinoctial Orbital Elements (M-GEqOEs) is defined as

$$\{\tilde{p},\ p_1,\ p_2,\ q_1,\ q_2,\ L\}. \tag{1}$$

The first element in the M-GEqOE set is the generalized semi-latus rectum, $\tilde{p}$, determined as

$$\tilde{p} = \frac{\tilde{h}^2}{\mu_C}\ . \tag{2}$$

The variables $\tilde{h}$ and $\mu_C$ represent the generalized angular momentum and the gravitational parameter associated with the central gravitational body. The former quantity is a function of the effective potential energy that is embedded with any necessary conservative perturbations.[3] The sixth element in the M-GEqOE set is the classical true longitude, $L$, which represents the time-varying or "fast" variable along the orbit. The true longitude is determined as

$$L = \omega + \Omega + \theta\ , \tag{3}$$

where $\theta$ is the classical true anomaly, and $\omega$ and $\Omega$ denote the argument of periapsis and the right ascension of ascending node, respectively. The second and third elements parameterize the eccen-

tricity vector and are defined as

$$p_1 = \tilde{e} \sin \Psi \tag{4}$$

$$p_2 = \tilde{e} \cos \Psi \ . \tag{5}$$

Here, the angle $\Psi$ denotes the generalized longitude of periapsis and is determined as

$$\Psi = L - \tilde{\theta} \ , \tag{6}$$

where $\tilde{\theta}$ is the generalized true anomaly. Finally, the elements $q_1$ and $q_2$ orient the equinoctial reference frame relative to the inertial reference frame. These elements are functions of the classical inclination, $i$, and the classical right ascension of the ascending node, $\Omega$, expressed as

$$q_1 = \tan \frac{i}{2} \sin \Omega \tag{7}$$

$$q_2 = \tan \frac{i}{2} \cos \Omega \ . \tag{8}$$

With the M-GEqOE set defined, the time derivatives for elements are detailed, providing a general form that may accommodate any perturbing forces.

Consider an inertial reference frame, denoted $\Sigma$, centered on a celestial body and defined as

$$\Sigma = \{O;\ \boldsymbol{e}_x,\ \boldsymbol{e}_y,\ \boldsymbol{e}_z\} \ . \tag{9}$$

Here, $\boldsymbol{e}_x = [1,\ 0,\ 0]^T$, $\boldsymbol{e}_y = [0,\ 1,\ 0]^T$, and $\boldsymbol{e}_z = [0,\ 0,\ 1]^T$. The spacecraft's orbital reference frame, denoted $\Sigma_{or}$, is defined by the orthonormal basis,

$$\Sigma_{or} = \{O;\ \boldsymbol{e}_r,\ \boldsymbol{e}_f,\ \boldsymbol{e}_h\} \ , \tag{10}$$

where $\boldsymbol{e}_r$ points along the spacecraft position vector, $\boldsymbol{e}_h$ is directed along the angular momentum vector, and $\boldsymbol{e}_f$ completes the dextral orthonormal triad

$$\boldsymbol{e}_r = \frac{\boldsymbol{r}}{r} \ , \quad \boldsymbol{e}_f = \boldsymbol{e}_h \times \boldsymbol{e}_r \ , \quad \text{and} \quad \boldsymbol{e}_h = \frac{\boldsymbol{r} \times \dot{\boldsymbol{r}}}{|\boldsymbol{r} \times \dot{\boldsymbol{r}}|} = \frac{\boldsymbol{h}}{h} \ . \tag{11}$$

Let the total perturbing force acting on the spacecraft be represented as

$$\boldsymbol{F} = \boldsymbol{P} - \nabla U \ , \tag{12}$$

where $\boldsymbol{P}$ represents the perturbing forces that are not modeled as a potential, and $-\nabla U$ models the contribution of forces derived from a potential energy, $U$. Projections of the total perturbing force and the external perturbing force term, denoted $\boldsymbol{P}$, into the orbital reference frame are given as

$$F_r = \boldsymbol{F} \cdot \boldsymbol{e}_r \ , \quad F_f = \boldsymbol{F} \cdot \boldsymbol{e}_f \ , \quad \text{and} \quad F_h = \boldsymbol{F} \cdot \boldsymbol{e}_h \ , \tag{13}$$

$$P_r = \boldsymbol{P} \cdot \boldsymbol{e}_r \ , \quad P_f = \boldsymbol{P} \cdot \boldsymbol{e}_f \ , \quad \text{and} \quad P_h = \boldsymbol{P} \cdot \boldsymbol{e}_h \ . \tag{14}$$

Additionally, the angular velocity of the equinoctial reference frame, $\Sigma_{eq}$, with respect to the inertial frame, $\Sigma$, is projected onto the equinoctial axes as

$$w_X = F_h \frac{r}{h} \cos L \tag{15}$$

$$w_Y = F_h \frac{r}{h} \sin L \tag{16}$$

$$w_Z = -F_h \frac{r}{h} \tan \frac{i}{2} \sin \omega + \theta \ . \tag{17}$$

Other quantities necessary to compute the time derivatives of the M-GEqOEs include the rate of change of the total energy of the system, which is evaluated as

$$\dot{\mathcal{E}} = \frac{\partial U}{\partial t} + \dot{r}P_r + \frac{h}{r}P_f \ . \tag{18}$$

Then, the general form of the time derivatives of the M-GEqOEs is given as

$$\begin{aligned}
\dot{\tilde{p}} &= \frac{2\tilde{h}}{\mu_C}\left[\frac{r^2\dot{\mathcal{E}}}{\tilde{h}} + \frac{r\dot{r}}{\tilde{h}}(2U - rF_r)\right] \\
\dot{p}_1 &= p_2\left(\frac{h-\tilde{h}}{r^2} - w_h\right) + \frac{1}{\tilde{h}}\left(\frac{X}{\tilde{a}} + 2p_2\right)(2U - rF_r) + \frac{1}{\tilde{h}^2}\left[Y(r+\tilde{p}) + r^2 p_1\right]\dot{\mathcal{E}} \\
\dot{p}_2 &= p_1\left(w_h - \frac{h-\tilde{h}}{r^2}\right) - \frac{1}{\tilde{h}}\left(\frac{Y}{\tilde{a}} + 2p_1\right)(2U - rF_r) + \frac{1}{\tilde{h}^2}\left[X(r+\tilde{p}) + r^2 p_2\right]\dot{\mathcal{E}} \\
\dot{q}_1 &= \frac{1}{2}w_Y\left(1 + q_1^2 + q_2^2\right) \\
\dot{q}_2 &= \frac{1}{2}w_X\left(1 + q_1^2 + q_2^2\right) \\
\dot{L} &= \frac{h}{r^2} + \frac{r}{h}F_h \tan\left(\frac{i}{2}\right)\sin\left(\omega + \theta\right) \ .
\end{aligned} \tag{19}$$

Any significant perturbations, modeled as a potential or otherwise, that are essential for modeling spacecraft dynamics are, thus, directly incorporated into the generalized elements and their time derivatives.

### Modeling Cislunar Dynamics

As spacecraft and other objects traverse cislunar space, their complex dynamical motion is influenced by the gravitational forces of the Earth and the Moon. Therefore, in addition to the dominant gravitational influence of one body, the gravitational perturbations caused by the other must be accounted for in trajectory design and prediction. In addition to that, solar gravity must be included to accurately represent the true dynamical environment.[6] Thus, for cislunar state propagation employing the M-GEqOEs, the gravitational influences of the Earth, Moon, and Sun are incorporated into the element set. Third-body perturbations by either the Earth or the Moon are embedded as a perturbing potential, where the potential energy associated with the perturbing force is given as[7]

$$U_{_P} = \mu_{_P}\left(\frac{1}{r_{_{Psc}}} - \frac{\boldsymbol{r}\cdot\boldsymbol{r}_{_{CP}}}{r_{_{CP}}^3}\right) \ , \tag{20}$$

where $\boldsymbol{r}$ represents the position vector from the central body to the spacecraft, and the subscripts $C$ and $P$ represent the central and perturbing bodies, respectively. Equation (20) may be rewritten as a convergent series of Legendre polynomials

$$U_{_P} = \frac{\mu_{_P}}{r_{_{CP}}}\left[1 + \sum_{k=2}^{k=\infty}\left(\frac{r}{r_{_{CP}}}\right)^k P_k(\cos\alpha)\right] \ , \tag{21}$$

where $\alpha$ is the angle between the position vectors $\boldsymbol{r}$ and $\boldsymbol{r}_{_{CP}}$, and $P_k$ represent Legendre polynomials.[7] The perturbing acceleration takes the form

$$-\nabla U_{_P} = \frac{\mu_{_P}}{r_{_{CP}}^2} \sum_{k=1}^{k=\infty} \left(\frac{r}{r_{_{CP}}}\right)^k \left[P'_{k+1}(\cos\alpha)\boldsymbol{e}_{\boldsymbol{r}_{_{CP}}} - P'_k(\cos\alpha)\boldsymbol{e}_{\boldsymbol{r}}\right] , \tag{22}$$

where $\boldsymbol{e}_{\boldsymbol{r}_{_{CP}}}$ and $\boldsymbol{e}_{\boldsymbol{r}}$ are the unit vectors along $\boldsymbol{r}_{_{CP}}$ and $\boldsymbol{r}$ respectively. In addition to that, the point mass gravity effects of the Sun are also considered in the current work. However, noting the numerical instabilities resulting from the use of true solar ephemerides, the gravity of the Sun is incorporated as an external perturbing force.[1] Nevertheless, these effects do manifest directly in the equations that evolve the M-GEqOEs, as indicated in Equation (19). In all cases, the locations of the celestial bodies are retrieved from the DE440 planetary ephemerides supplied by NASA Jet Propulsion Lab (JPL) Navigation and Ancillary Information Facility (NAIF).[8]

## UNCERTAINTY PROPAGATION AND CHARACTERIZATION

Previous work has demonstrated success in using the GEqOEs and M-GEqOEs for uncertainty propagation along various cislunar orbits. Measured improvements in the preservation of Gaussian behavior are demonstrated for the case when Earth-Moon dynamics are considered.[4,9] In the current work, the evolution of uncertainty under high-fidelity dynamics in the generalized coordinates via the M-GEqOE set is explored.

### Methodology

The current work employs two methods for propagating the uncertainty along each orbit. The first is Monte Carlo analysis to obtain a representation of the *true* probability distribution along the selected orbits in both Cartesian and generalized coordinates. The second methodology is the Unscented Transform (UT), which is employed to obtain the initial uncertainty in generalized coordinates.[2,10] In addition, the UT serves as a means of approximating the moments of the true probability distribution at each time step.[4]

*Monte Carlo Analysis* In the current work, Monte Carlo analysis utilizes $N = 10,000$ samples for all simulations to facilitate analysis while maintaining computational feasibility. For uncertainty propagated in Cartesian coordinates, each sample is propagated using the $n$-body ephemeris model for one revolution.[5] Similarly, the M-GEqOE equations of motion embedded with lunar gravity perturbations, and with solar gravity modeled as an external perturbing force, are propagated for $N$ samples for the same time. At each time step, then, the mean and covariance for either scenario are computed as

$$\boldsymbol{m}_x(t) = \frac{1}{N}\sum_{i=1}^{N} \boldsymbol{x}_i(t) \quad \text{and} \quad \boldsymbol{P}_{xx}(t) = \frac{1}{N}\sum_{i=1}^{N} \left(\boldsymbol{x}_i(t) - \boldsymbol{m}_x(t)\right)\left(\boldsymbol{x}_i(t) - \boldsymbol{m}_x(t)\right)^T , \tag{23}$$

where $\boldsymbol{x}_i(t)$ is the state of the $i^{\text{th}}$ sample at time $t$. The mean and covariance computed via Monte Carlo methods serve as a benchmark for comparing other approaches that aim to approximate these statistical moments.

*Unscented Transform* The Unscented Transform (UT) is a methodology for deterministically sampling a fixed number of points, termed sigma points, to approximate the mean and covariance

of some given distribution.[11] Consider some nonlinear transformation represented as

$$\boldsymbol{y} = \boldsymbol{g}(\boldsymbol{x}) \,, \tag{24}$$

where $\boldsymbol{x}$ is Gaussian. The mean and covariance of $\boldsymbol{x}$ are known and denoted as $\boldsymbol{m}_x$ and $\boldsymbol{P}_{xx}$, respectively. The pdf of $\boldsymbol{x}$ is, thus, expressed as $p(\boldsymbol{x}) = p_g\left(\boldsymbol{x}; \boldsymbol{m}_x, \boldsymbol{P}_{xx}\right)$. Assuming $\boldsymbol{x} \in \mathbb{R}^n$, $2n+1$ sigma points are drawn and given as

$$\boldsymbol{\mathcal{X}}^{(0)} = \boldsymbol{m}_x, \quad \boldsymbol{\mathcal{X}}^{(i)} = \boldsymbol{m}_x + \sqrt{n+\lambda}\left[\boldsymbol{S}_{xx}\right]_i, \quad \text{and} \quad \boldsymbol{\mathcal{X}}^{(i+n)} = \boldsymbol{m}_x - \sqrt{n+\lambda}\left[\boldsymbol{S}_{xx}\right]_i \,, \tag{25}$$

where $i = 1, ..., n$.[12] The quantity $\left[\boldsymbol{S}_{xx}\right]_i$ is the $i^{\text{th}}$ column of the matrix $\boldsymbol{S}_{xx}$, determined such that $\boldsymbol{P}_{xx} = \boldsymbol{S}_{xx}\boldsymbol{S}_{xx}^T$. The nonlinear transformation in Equation (24) is then applied to each sigma point, yielding the transformed sigma points

$$\boldsymbol{\mathcal{Y}}^{(i)} = \boldsymbol{g}\big(\boldsymbol{\mathcal{X}}^{(i)}\big) \,, \tag{26}$$

where $i = 0, ..., 2n$. Next, the scaling parameter $\lambda$ is computed as

$$\lambda = \alpha^2\left(n + \kappa\right) - n \,, \tag{27}$$

where $\alpha$ and $\kappa$ dictate the spread of the sigma points around the mean.[13] For this investigation, $n = 6$, and $\alpha = 1$ and $\kappa = -3$ are selected as the user-defined parameters. Next, the mean and covariance weights associated with each point are computed

$$w_m^{(0)} = \frac{\lambda}{n+\lambda} \quad \text{and} \quad w_m^{(i)} = \frac{1}{2\left(n+\lambda\right)} \tag{28}$$

$$w_c^{(0)} = \frac{\lambda}{n+\lambda} + \left(1 - \alpha^2 + \beta\right) \quad \text{and} \quad w_c^{(i)} = \frac{1}{2\left(n+\lambda\right)} \tag{29}$$

$\forall\ i = 1, ..., 2n$. The subscripts $m$ and $c$ denote the mean and covariance weights, respectively. The parameter $\beta$ is used to incorporate prior information and is set equal to two in the current work.[11] Together with the mean and covariance weights, the transformed sigma points are used to approximate the mean and covariance as

$$\boldsymbol{m}_y \approxeq \sum_{i=0}^{2n} w_m^{(i)} \boldsymbol{\mathcal{Y}}^{(i)} \quad \text{and} \quad \boldsymbol{P}_{yy} \approxeq \sum_{i=0}^{2n} w_c^{(i)} \left(\boldsymbol{\mathcal{Y}}^{(i)} - \boldsymbol{m}_y\right)\left(\boldsymbol{\mathcal{Y}}^{(i)} - \boldsymbol{m}_y\right)^T \,. \tag{30}$$

For each point along the orbit, the mean and covariance computed via the UT method approximate the true pdf as a Gaussian distribution.

**Bhattacharyya Coefficient**

The Bhattacharyya coefficient is a measure of the statistical similarity between two distributions.[14] While other options for assessing statistical similarity, such as the Mahalanobis distance[2] and the Kullback-Leibler divergence[4,9] have been explored, the Bhattacharyya coefficient offers a bounded measure that can be leveraged for comparison across different coordinates and measurement scales.[15] The Bhattacharyya coefficient between two distributions $p(\boldsymbol{x})$ and $q(\boldsymbol{x})$ is determined as

$$BC(p, q) = \int \sqrt{p(\boldsymbol{x})q(\boldsymbol{x})}\mathrm{d}\boldsymbol{x} \,. \tag{31}$$

For two identical distributions, the value of the coefficient is unity; a value of zero indicates total dissimilarity between the distributions. While the coefficient admits a closed form for the case of two Gaussian distributions, the general form in Equation (31) is valid for all distribution types.[16] In the current work, Equation (31) is rewritten to evaluate the Bhattacharyya coefficient as an expectation taken with respect to $p(\boldsymbol{x})$. To that end, multiply and divide the integrand in Equation (31) by $\sqrt{p(\boldsymbol{x})}$ as

$$BC(p,q) = \int \sqrt{\frac{p(\boldsymbol{x})}{p(\boldsymbol{x})}}\sqrt{p(\boldsymbol{x})q(\boldsymbol{x})}\mathrm{d}\boldsymbol{x} \tag{32}$$

$$= \int p(\boldsymbol{x})\sqrt{\frac{q(\boldsymbol{x})}{p(\boldsymbol{x})}}\mathrm{d}\boldsymbol{x} \tag{33}$$

$$= \mathbb{E}_{p(\boldsymbol{x})}\left\{\sqrt{\frac{q(\boldsymbol{x})}{p(\boldsymbol{x})}}\right\} . \tag{34}$$

The expectation integral is then determined via Monte Carlo integration as

$$BC(p,q) \approx \frac{1}{N}\sum_{i=1}^{N}\left(\sqrt{\frac{q(\boldsymbol{x}_i)}{p(\boldsymbol{x}_i)}}\right) . \tag{35}$$

It is noted that Equation (35) requires the pdfs of the two distributions. In the current work, $q(\boldsymbol{x})$ is known and assumed to be Gaussian, i.e., $q(\boldsymbol{x}) = p_g(\boldsymbol{x}; \boldsymbol{m}, \boldsymbol{P})$, where $\boldsymbol{m}$ and $\boldsymbol{P}$ are obtained via the UT. The pdf $p(\boldsymbol{x})$ represents the true distribution, the exact form of which is not known. One methodology for obtaining a reasonable approximation of $p(\boldsymbol{x})$ is by fitting a Gaussian Mixture Model (GMM) to the particle set that represents the truth. The pdf representing the true distribution is then expressed as

$$p(\boldsymbol{x}) = \sum_{\ell=1}^{L} w^{(\ell)} p_g\left(\boldsymbol{x}; \boldsymbol{m}_x^{(\ell)}, \boldsymbol{P}_{xx}^{(\ell)}\right) , \tag{36}$$

where $L$ is the number of GMM components, and $w^{(\ell)}$, $\boldsymbol{m}_x^{(\ell)}$, and $\boldsymbol{P}_{xx}^{(\ell)}$ represent the weight, mean, and covariance of the $\ell^{\text{th}}$ component.[17] While the number of components is variable, unless otherwise noted, the current work assumes $L = 20$ components for modeling the true distributions. Thus, at each time step for a given orbit, the Bhattacharyya coefficient between the GMM and Gaussian distributions that represent the true and approximate pdfs, respectively, is determined. Insight into the error introduced by approximating the true distribution as a Gaussian distribution is obtained, where lower values of the Bhattacharyya coefficient indicate greater deviation from Gaussian behavior.

## RESULTS

State and uncertainty propagation under high-fidelity dynamics are assessed for a variety of cislunar orbits that traverse various regions within this domain. For each orbit, the states are evolved in generalized coordinates and, via transformation into Cartesian coordinates, compared against the solution obtained via Cowell's method. For either propagation methodology, the Earth-Moon-Sun point mass gravitational forces are modeled. In addition to state propagation, the evolution of uncertainty along each trajectory is assessed. To maintain the scope of this work as the characterization

of downstream probability distributions, a single revolution of each cislunar trajectory is considered for uncertainty propagation.

### 9:2 Near Rectilinear Halo Orbit

As one example, the $9{:}2$ Near Rectilinear Halo Orbit (NRHO), which is the baseline orbit for NASA's upcoming Gateway lunar outpost,[18] is considered. The dynamics that govern the motion of a spacecraft in this orbit are highly nonlinear, and unmodeled perturbations may induce significant deviation from the baseline trajectory over time. The NRHO is propagated using the M-GEqOE equations, along with the conventional Cartesian methodology, for one revolution of the orbit or approximately $6.5\ days$. The results are plotted in Figure 1, where the M-GEqOE solution appears in blue, while the Cartesian propagation appears in orange, in both the Earth-Moon rotating and Moon-centered inertial frames. While the Cartesian representations of the two solutions indicate visual consistency between the results, the error in position and velocity confirms the accuracy of the M-GEqOE solution, plotted in Figure 1(c). There is a noticeable spike in the error at perilune, after which the error in both quantities returns to a nominal value. It is also noted that the magnitudes of error between the two methodologies observed in Figure 1(c) are similar to the values seen under Earth-Moon CR3BP dynamics for this orbit.[3] Thus, even though the pulsation of the Earth-Moon distance and solar gravity significantly perturb the orbit relative to the CR3BP solution, the M-GEqOEs are able to capture those perturbations without loss of accuracy.

Next, the evolution of uncertainty along the NRHO is assessed for the M-GEqOEs and compared against propagation in Cartesian coordinates. At the initial time, which occurs at apolune, $1\sigma$ values of uncertainty of $10\ km$ and $0.1\ m/s$ are assumed along the position and velocity channels, respectively. Uncertainty is then evaluated at each point along the orbit for approximately $6.5\ days$. Figure 2(a) illustrates the Bhattacharyya coefficient between the true and approximating distributions for the generalized coordinates (blue) and Cartesian coordinates (orange). Evidently, despite the high-fidelity dynamical modeling, a Gaussian approximation of the true distribution is reasonably accurate for both representations at most locations along the orbit. Distinct deviation from Gaussian behavior is observed at around $3.25\ days$, corresponding to passage along perilune. While both representations exhibit departure from the nominal, the degree of non-Gaussianity seen in the Cartesian case is significantly greater than the M-GEqOE methodology. Thus, a Gaussian approximation of the truth induces a smaller error in uncertainty characterization in generalized coordinates. This result is further validated by visualizing the uncertainty clouds at perilune for both coordinates. Figure 2(b) illustrates pairs plots for the M-GEqOE (blue, upper triangle) and Cartesian (orange, lower triangle) methodologies. In each subplot, the ellipses indicate the $1,\ 2$, and $3\sigma$ uncertainty intervals associated with the Gaussian approximation of the true distributions. Clearly, a majority of the Monte Carlo samples are captured for the M-GEqOE case, whereas in the Cartesian case, the curvature of the true distribution is not captured by a Gaussian approximation.

### Earth-Centered Sidereal Resonant Orbit

Another cislunar orbit that is considered in this investigation is an Earth-centered sidereal resonant orbit. Despite being centered on the Earth, this orbit possesses a relatively high apogee radius and, thus, perturbations from lunar gravity are non-negligible. The selected orbit is identified from the family of $4{:}1$ Earth-Moon sidereal resonant orbits and possesses a period of approximately $27.30\ days$ in the rotating frame, rendering it to be in approximate sidereal resonance with the Moon.[5] Thus, four revolutions of the orbit as viewed in the inertial frame represent one

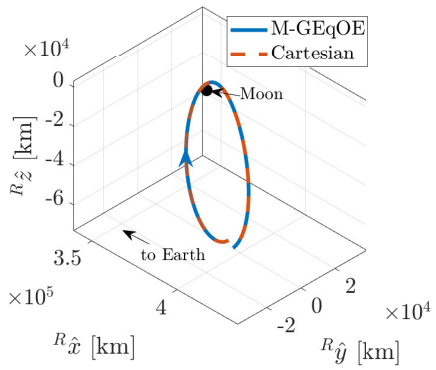


(a) Earth-Moon rotating frame

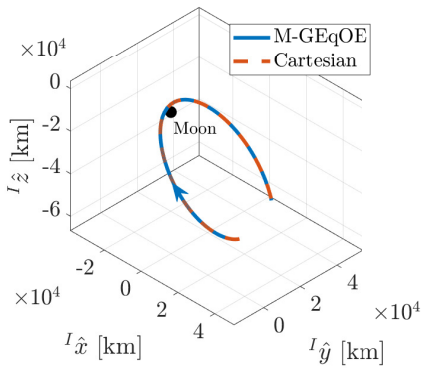


(b) Moon-centered inertial frame

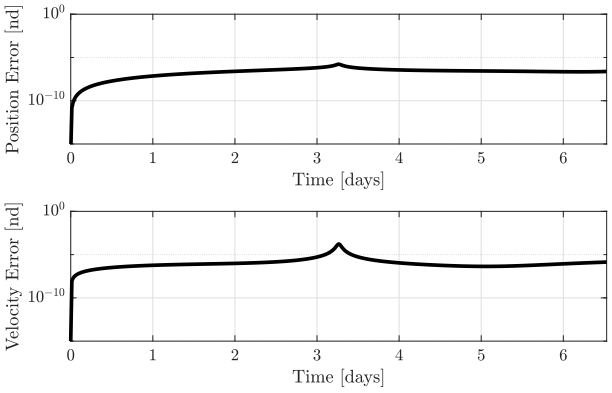


(c) Position and Velocity Errors

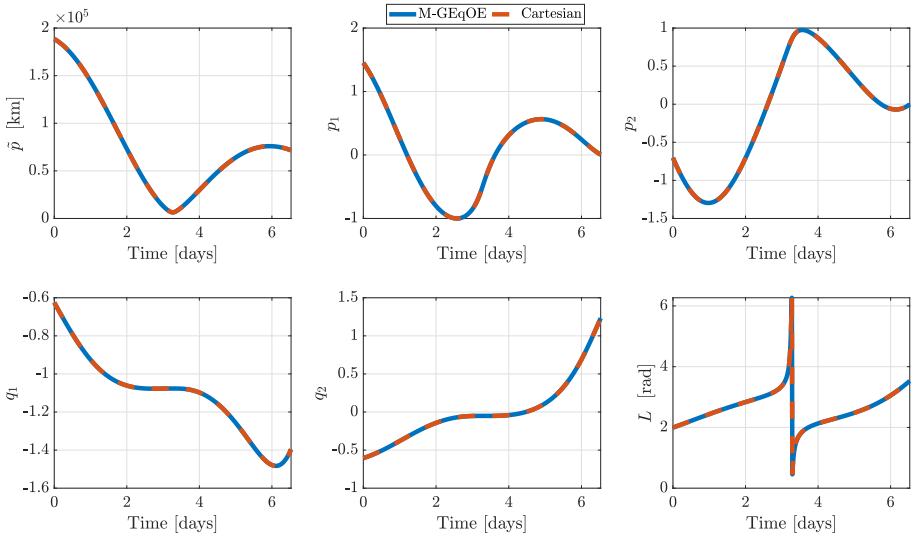


(d) Evolution of M-GEqOEs

**Figure 1. Cartesian and M-GEqOE representations of the 9:2 NRHO over one revolution. Blue and orange curves represent solutions propagated in the M-GEqOE and Cartesian coordinates, respectively.**

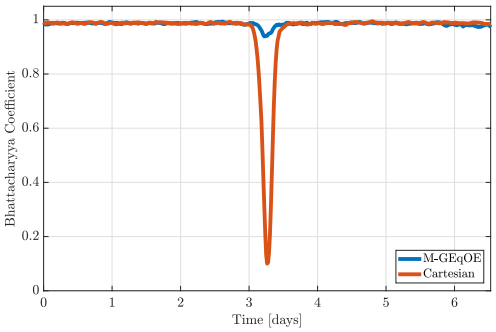


(a) Bhattacharyya coefficient

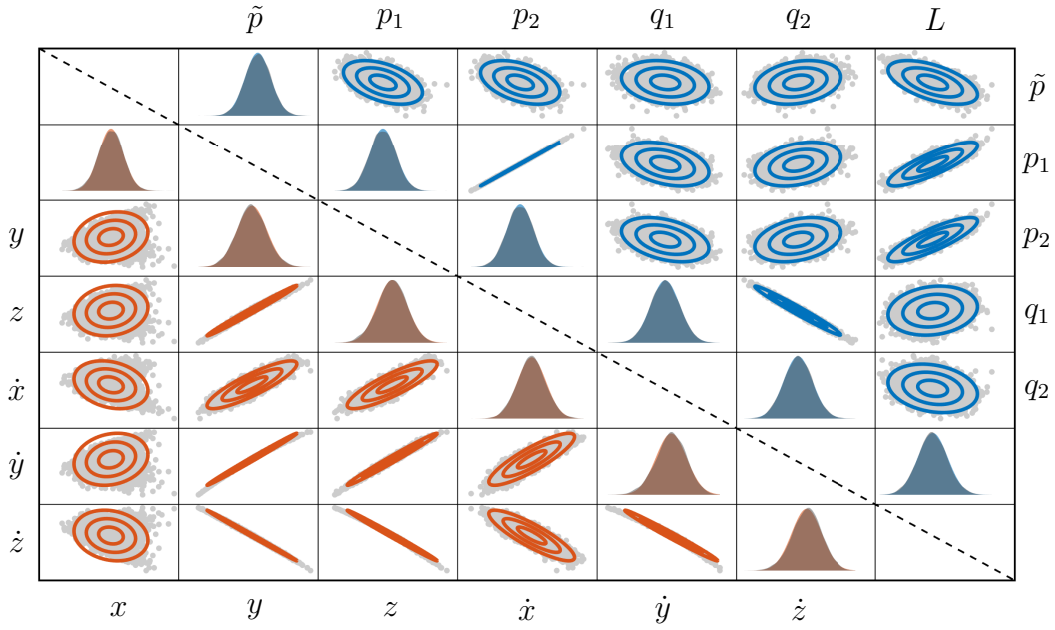


(b) Pairs plot

**Figure 2. Bhattacharyya coefficient evaluated over one revolution, and pairs plot at $t = 3.25\ days$ for the 9:2 NRHO with uncertainty propagated in Cartesian (lower triangular) and M-GEqOE (upper triangular) coordinates.**

"closed" orbit in the rotating frame. For this analysis, the initial states for the orbit are evolved under Earth-Moon-Sun dynamics using the M-GEqOE and Cartesian equations of motion. The solution obtained via the M-GEqOE methodology is transformed into Cartesian coordinates and appears in Figures 3(a) and 3(b) as viewed in the Earth-Moon rotating and Earth-centered inertial frames. The resulting blue solution curve closely matches the trajectory obtained via direct propagation in Cartesian coordinates. Figure 3(c) illustrates the error in position and velocity from the two methods of propagation and confirms the accuracy of the high-fidelity M-GEqOE propagator. Finally, the Cartesian solution is transformed into the generalized coordinates, as demonstrated in Figure 3(d). The consistency between the values of each orbital element over time is noted.

The evolution of uncertainty along the 4:1 resonant orbit is assessed over one revolution in both coordinates. For this orbit as well, the initial $1\sigma$ values of uncertainty are $10\ km$ and $0.1\ m/s$ along

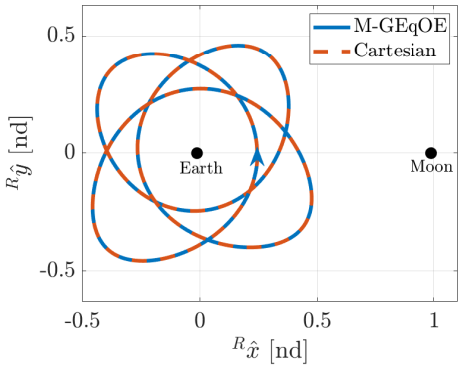


(a) Earth-Moon rotating frame

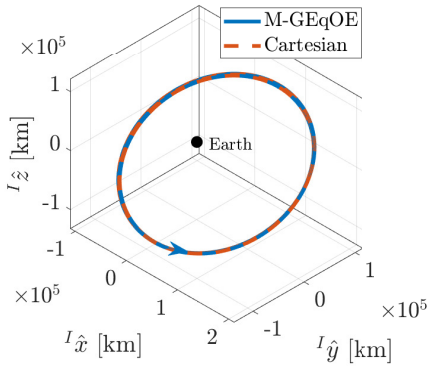


(b) Earth-centered inertial frame

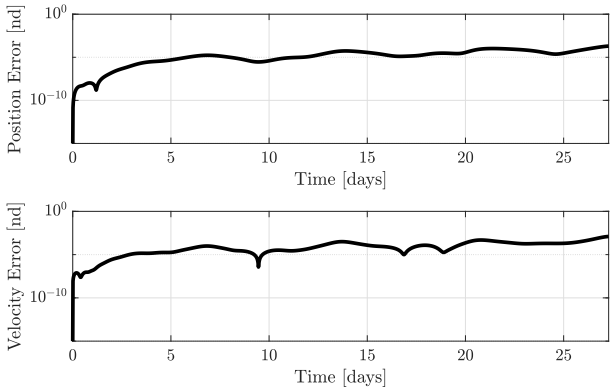


(c) Position and Velocity Errors

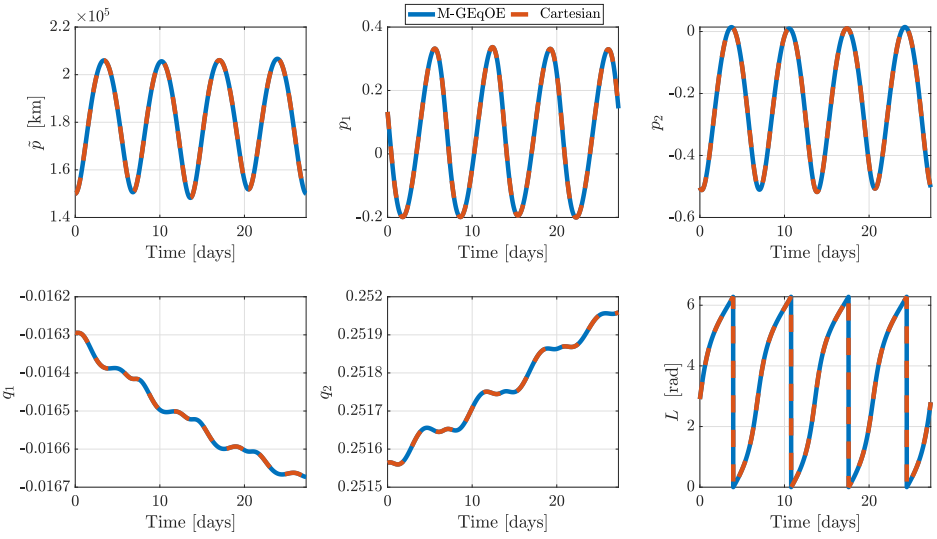


(d) Evolution of M-GEqOEs

**Figure 3. Cartesian and M-GEqOE representations of the 4:1 resonance over one revolution. Blue and orange curves represent solutions propagated in the M-GEqOE and Cartesian coordinates, respectively.**

the position and velocity components. In both the M-GEqOE and Cartesian coordinates, for each point in time, the true pdf is determined via Monte Carlo sampling and propagation. A Gaussian approximation of the true pdf, supplied by the UT, is employed to assess the Gaussianity of the truth. Figure 4(a) illustrates the Bhattacharyya coefficient between the true and approximating pdfs at each point, where the blue curve represents uncertainty evolved in M-GEqOE coordinates, and the orange curve represents the Cartesian methodology. Distinct dips in the value of the Bhattacharyya coefficient are seen for both scenarios. The locations of these dips, that indicate departure from Gaussian behavior, correspond to perigee and occur approximately every $6.8\ days$. Uncertainty evolved in M-GEqOE coordinates represents a smaller deviation from the nominal Gaussian representation, while uncertainty in Cartesian coordinates devolves rapidly. However, it is also noted that the performance of the M-GEqOE methodology degrades with each perigee pass. Nonetheless, the degree to which those nonlinearities manifest is significantly less than in Cartesian coordinates. To further intuit these observations, Figure 4(b) illustrates the uncertainty clouds in both coordinates at the first perigee pass, $6.8\ days$ into the propagation. The projections in the M-GEqOE coordinates (blue) exhibit the onset of non-Gaussian behavior along some projections. In contrast, the Cartesian coordinates (orange) exhibit pronounced curvature along all projections of the particle cloud.

**Elliptic Lunar Frozen Orbit**

As a third example for high-fidelity state and uncertainty propagation in the cislunar domain, consider an Elliptic Lunar Frozen Orbit (ELFO) for operations in the lunar vicinity, including potentially hosting data relay constellations.[19] These orbits are characterized by high values of inclination, eccentricity, and altitude, allowing long-term coverage of the lunar south pole. More recently, extensive research has been done to refine these orbits for rapid constellation design in a higher-fidelity dynamical environment.[20,21] In the current work, the initial conditions of a representative ELFO, as provided by Park et al.,[21] are used for analysis. The initial state is transformed into the generalized coordinates for high-fidelity propagation over $30\ days$ using the M-GEqOE equations. The resulting solution, along with the trajectory obtained via direct Cartesian propagation, appears in Figures 5(a) and 5(b) as viewed in the Earth-Moon rotating and Moon-centered inertial frames. The accuracy of the M-GEqOE solution is confirmed via Figure 5(c), which illustrates the error in position and velocity over $30\ days$. Figure 5(d) illustrates the M-GEqOEs that characterize the ELFO, where the orange curves represent the Cartesian-propagated states transformed into the generalized coordinates. As expected, periodic and secular drift in the elements is observed under high-fidelity propagation.

To assess the evolution of uncertainty along the selected ELFO, initial $1\sigma$ uncertainty values of $1\ km$ and $0.01\ m/s$ are assumed along the position and velocity components. Additionally, while initial analysis assumed a 20-component GMM to model the true distribution in both sets of coordinates to maintain consistency with the other orbits, the number of components is increased to $50$ to better fit the particle sets. The Bhattacharyya coefficient is computed to compare the resulting true pdf against its Gaussian approximation in both generalized and Cartesian coordinates, represented in Figure 6(a). The M-GEqOE methodology is able to retain a Gaussian approximation for approximately $1\ day$, whereas the Cartesian approach diverges rapidly early on. Beyond that point, Gaussian approximations no longer accurately represent the true pdf in either coordinate set, though the discrepancy is less severe in the generalized coordinates compared to the Cartesian case. Note that the focus of uncertainty analysis for this orbit is limited to $3\ days$ due to rapid loss of structure in the pdfs for both sets of coordinates over time given the initial levels of uncertainty. Finally, Figure 6(b) illustrates the uncertainty clouds for uncertainty propagated in the M-GEqOE (blue)

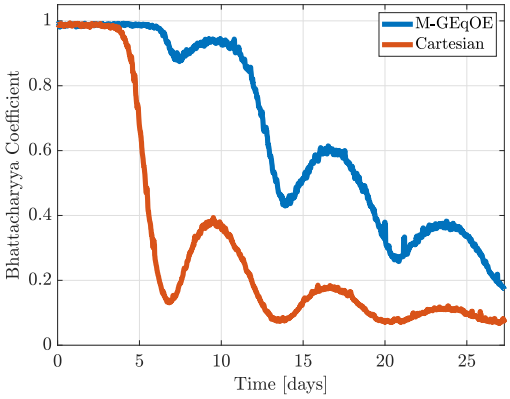


(a) Bhattacharyya coefficient

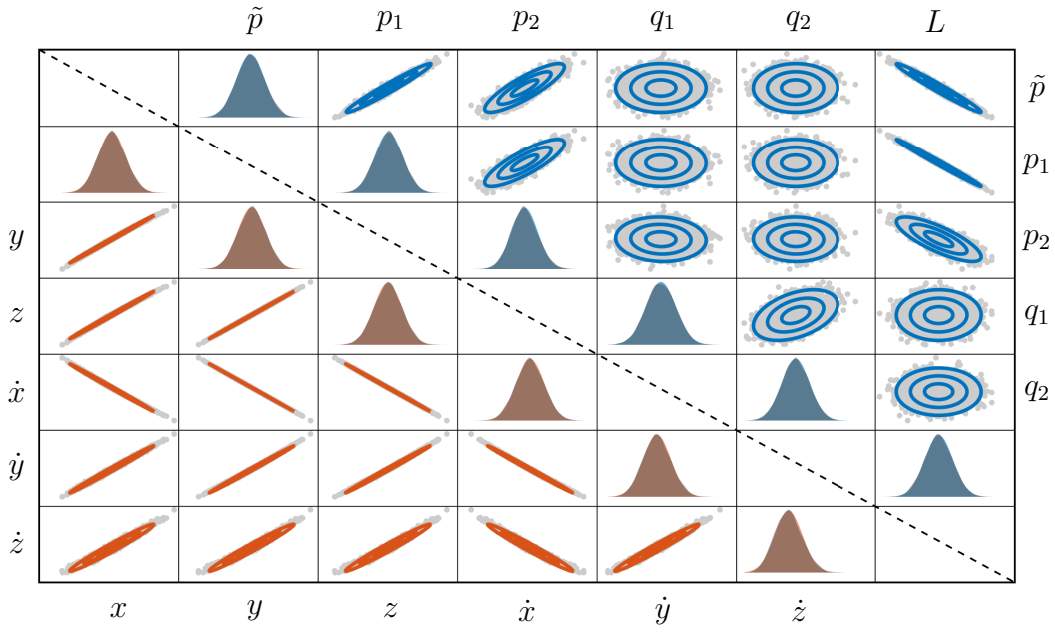


(b) Pairs plot

**Figure 4. Bhattacharyya coefficient evaluated over one revolution, and pairs plot at $t = 6.8\ days$ for the 4:1 sidereal resonance with uncertainty propagated in Cartesian (lower triangular) and M-GEqOE (upper triangular) coordinates.**

and Cartesian (orange) coordinates at $1.5\ days$ downstream. Evidently, deviation from Gaussian behavior is expected in both representations based on the value of the Bhattacharyya coefficient at this time. In the M-GEqOE coordinates, the Gaussian approximations reasonably capture the true distribution shape in most projections. On the other hand, the Cartesian coordinates exhibit significantly increased curvature and elongation for all pairs of components. These deviations from Gaussianity are consistent with the decline in the Bhattacharyya coefficient for the Cartesian case around this time.

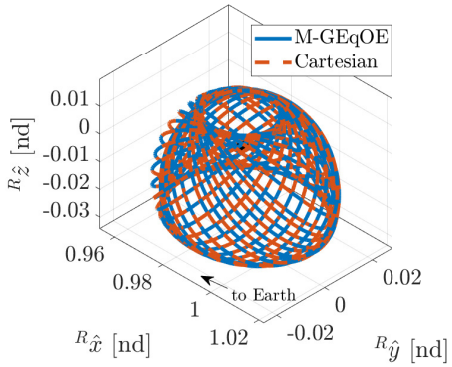


(a) Earth-Moon rotating frame

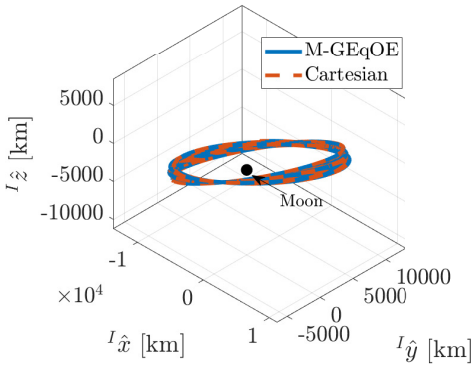


(b) Moon-centered inertial frame

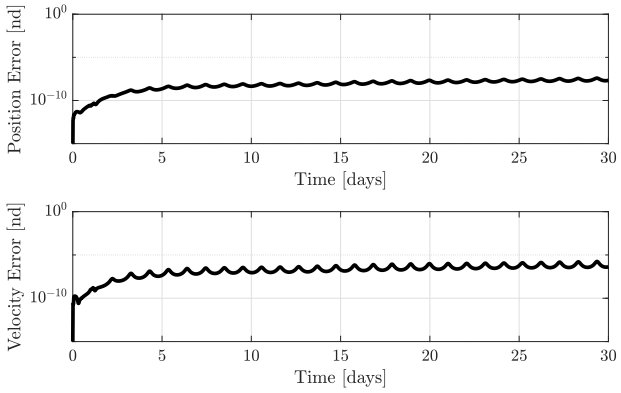


(c) Position and Velocity Errors

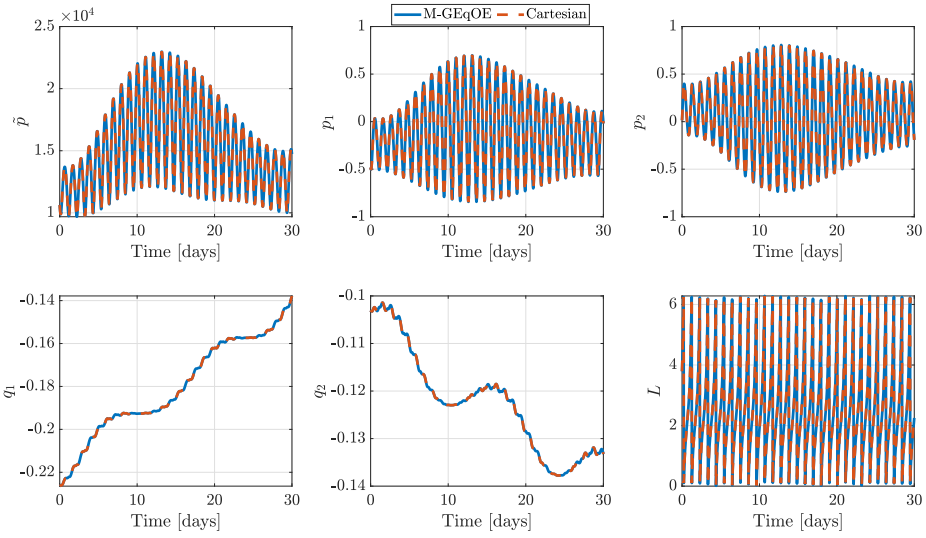


(d) Evolution of M-GEqOEs

**Figure 5. Cartesian and M-GEqOE representations of the ELFO over 30 $days$. Blue and orange curves represent solutions propagated in the M-GEqOE and Cartesian coordinates, respectively.**

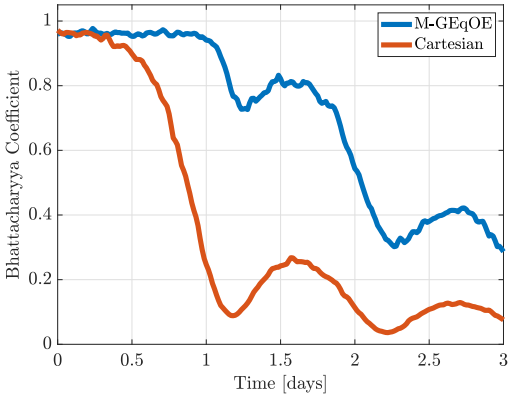


(a) Bhattacharyya coefficient

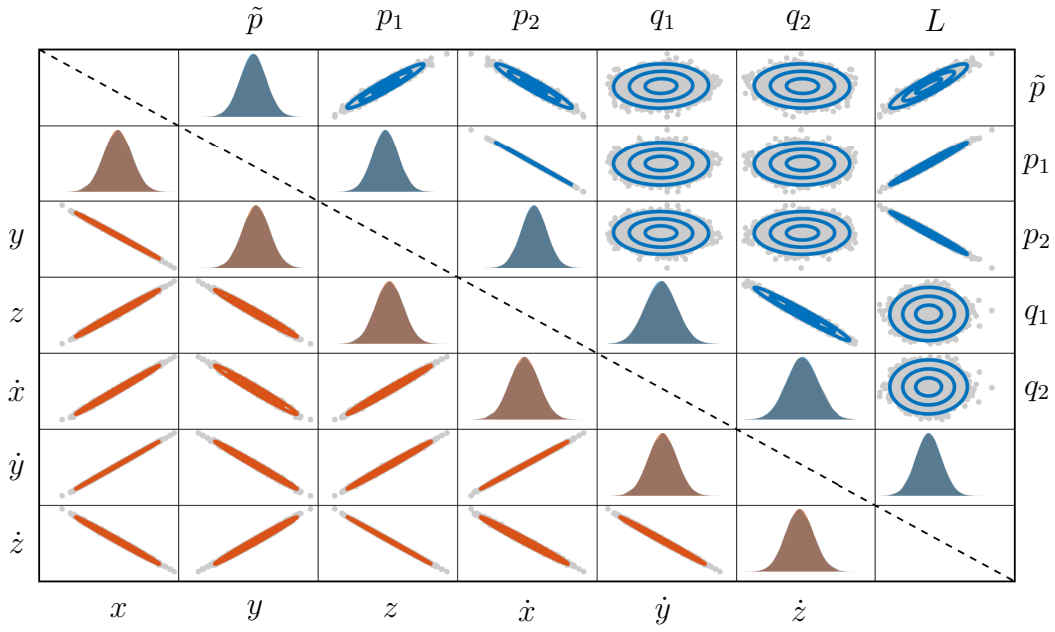


(b) Pairs plot

**Figure 6. Bhattacharyya coefficient evaluated over 3 $days$ and pairs plot at $t = 1.5$ $days$ for the ELFO with uncertainty propagated in Cartesian (lower triangular) and M-GEqOE (upper triangular) coordinates.**

## CONCLUDING REMARKS

Cislunar space poses a challenging dynamical environment that requires high-fidelity dynamical modeling to accurately predict spacecraft trajectories and associated uncertainties. In the current work, the Modified Generalized Equinoctial Orbital Elements (M-GEqOEs) are explored as an option for cislunar propagation under the presence of the necessary gravitational perturbations. The M-GEqOE set allows the direct inclusion of conservative perturbations, offering a low-complexity methodology for modeling dynamics in this complex regime. Various cislunar orbits are constructed to demonstrate the applicability of this element set for high-fidelity propagation under the gravita-

tional influence of the Earth, Moon, and Sun. In addition to state propagation, uncertainty characterization via the M-GEqOE set is explored for various cislunar orbits. For the orbits considered in this work, improved preservation of Gaussianity is observed via the M-GEqOE methodology, compared to conventional Cartesian propagation. In addition to exhibiting Gaussian behavior for longer propagation times, improved uncertainty characterization is observed at sensitive and highly nonlinear regions in the generalized coordinates.

## ACKNOWLEDGEMENTS

Feedback and discussions with members of the PROMETHEUS Lab at Texas A&M University are acknowledged. The authors appreciate valuable suggestions by Kyle Craft at SpaceX. Helpful discussions with John Iannamorelli at Draper are also appreciated.

## REFERENCES

[1] G. Baù, J. Hernando-Ayuso, and C. Bombardelli, "A Generalization of the Equinoctial Orbital Elements," *Celestial Mechanics and Dynamical Astronomy*, Vol. 133, Dec. 2021, 10.1007/s10569-021-10049-1.

[2] J. Hernando-Ayuso, C. Bombardelli, G. Baù, and A. Martínez-Cacho, "Near-Linear Orbit Uncertainty Propagation Using the Generalized Equinoctial Orbital Elements," *Journal of Guidance, Control, and Dynamics*, Vol. 46, No. 4, 2023, 10.2514/1.G006864.

[3] M. Gupta and K. J. DeMars, "Cislunar Astrodynamics Leveraging Generalized Equinoctial Orbital Elements," *AAS/AIAA Space Flight Mechanics Meeting*, Kaua'i, Hawaii, 2025.

[4] M. Gupta and K. J. DeMars, "Uncertainty Propagation for Cislunar Space Domain Awareness," *AAS/AIAA Space Flight Mechanics Meeting*, Kaua'i, Hawaii, 2025.

[5] M. Gupta, *Navigating Chaos: Resonant Orbits for Sustaining Cislunar Operations*. Ph.D. Dissertation, Purdue University, West Lafayette, Indiana, 2024.

[6] S. T. Scheuerle Jr., *Low-Energy Lunar Transfers in the Bicircular Restricted Four-Body Problem*. Ph.D. Dissertation, Purdue University, West Lafayette, Indiana, 2024.

[7] Battin, Richard H., *An Introduction to the Mathematics and Methods of Astrodynamics*. Reston, VA: American Institute of Aeronautics and Astronautics, 1999.

[8] R. S. Park, W. M. Folkner, J. G. Williams, and D. H. Boggs, "The JPL Planetary and Lunar Ephemerides DE440 and DE441," *The Astronomical Journal*, 2021, 10.3847/1538-3881/abd414.

[9] M. Gupta and K. J. DeMars, "Cislunar Space Domain Awareness using the Modified Generalized Equinoctial Orbital Eleents," *9th European Conference on Space Debris*, Bonn, Germany, 2025.

[10] K. W. McGee, "State and Uncertainty Propagation using Generalized Equinoctial Orbital Elements," M.S. Thesis, Texas A&M University, College Station, TX, Aug. 2023.

[11] S. Julier, "The Scaled Unscented Transformation," *Proceedings of the 2002 American Control Conference (IEEE Cat. No.CH37301)*, Vol. 6, 2002, 10.1109/ACC.2002.1025369.

[12] R. Zanetti and K. J. DeMars, "Joseph Formulation of Unscented and Quadrature Filters with Application to Consider States," *Journal of Guidance, Control, and Dynamics*, Vol. 36, No. 6, 2013, pp. 1860–1864, 10.2514/1.59935.

[13] R. van der Merwe, *Sigma-Point Kalman Filters for Probabilistic Inference in Dynamic State-Space Models*. Ph.D. Dissertation, Oregon Health and Science University, Portland, OR, 2004.

[14] A. Bhattacharyya, "On a Measure of Divergence between Two Multinomial Populations," *Sankhyā: The Indian Journal of Statistics (1933-1960)*, Vol. 7, No. 4, 1946, pp. 401–406.

[15] F. J. Aherne, N. A. Thacker, and P. I. Rockett, "The Bhattacharyya Metric as an Absolute Similarity Measure for Frequency Coded Data," *Kybernetika*, Vol. 34, No. 4, 1998, pp. [363]–368.

[16] S. Bi, S. Prabhu, S. Cogan, and S. Atamturktur, "Uncertainty Quantification Metrics with Varying Statistical Information in Model Calibration and Validation," *AIAA Journal*, Vol. 55, No. 10, 2017, pp. 3570–3583, 10.2514/1.J055733.

[17] K. J. DeMars, R. H. Bishop, and M. K. Jah, "Entropy-Based Approach for Uncertainty Propagation of Nonlinear Dynamical Systems," *Journal of Guidance, Control, and Dynamics*, Vol. 36, No. 4, 2013, pp. 1047–1057, 10.2514/1.58987.

[18] D. E. Lee, "Gateway Destination Orbit Model : A Continuous 15 Year NRHO Reference Trajectory," 2019. NASA Johnson Space Center White Paper.

[19] T. A. Ely and E. Lieb, "Constellations of Elliptical Inclined Lunar Orbits providing Polar and Global Coverage," *Journal of the Astronautical Sciences*, Vol. 54, No. 1, 2006, 10.1007/BF03256476.

[20] S. K. Singh, R. Woollands, E. Taheri, and J. Junkins, "Feasibility of Quasi-Frozen, Near-Polar and Extremely Low-Altitude Lunar Orbits," *Acta Astronautica*, Vol. 166, 2020, pp. 450–468, https://doi.org/10.1016/j.actaastro.2019.10.037.

[21] B. Park, K. C. Howell, and S. Stewart, "Elliptical Lunar Frozen Orbit Constellation Design within a Model of Evolving Fidelity," *AAS/AIAA Space Flight Mechanics Meeting*, Kaua'i, Hawaii, 2025.